Neural Network-Enhanced Reproducing Kernel Particle Method for Image-based Multiphysics Damage Modeling of Energy Storage Materials

Kristen Susuki[1,2], Jeffery Allen[2] , J.S. Chen[1]

[1] University of California San Diego, Department of Structural Engineering
[2] National Renewable Energy Laboratory, Computational Science Center

Center for Extreme Events Research

UC San Diego

NREL Transforming ENERGY

USNCCM17 Conference – Albuquerque, NM– July 26, 2023
NREL/PR-2C00-85039

Li-ion Battery Electrode Microstructures and Chemo-Mechanical Cracking

Electrode Microstructure and Chemo-mechanical Cracking

Cathode Composition:
- Randomly-oriented grains
- Anisotropic grain material properties

+

Charge Cycling:
- Li movement between electrodes causes nonuniform grain expansion and contraction

↓

Chemo-mechanical cracking:
- Inhibited Li flow via tortuous diffusion path
- Reduced battery life

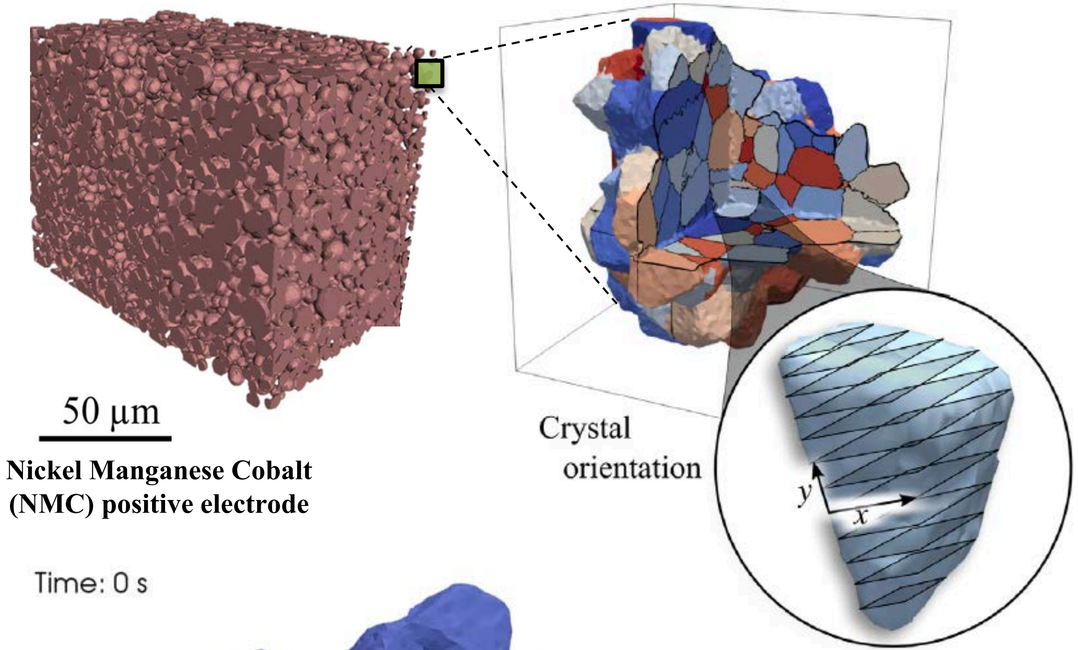

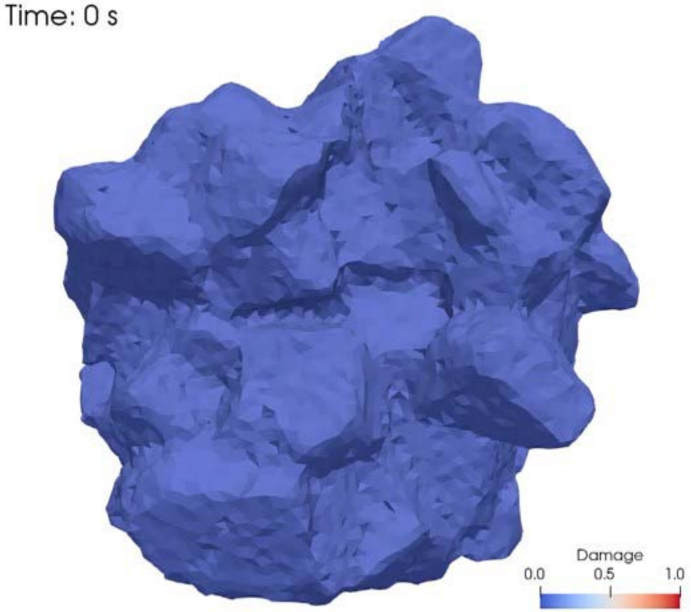

1. NREL. "Battery Microstructures Library." https://www.nrel.gov/transportation/microstructure.html.
2. Allen, J., P. Weddle, A. Verma, et al. 2021. "Quantifying the influence of charge rate and cathode-particle architectures on degradation of Li-ion cells through 3D continuum-level damage models." *J. Power Sources.* doi.org/10.1016/j.jpowsour.2021.230415.
3. Quinn, A., H. Moutinho, F. Usseglio-Viretta, et al. 2020. "Electron Backscatter Diffraction for Investigating Lithium-Ion Electrode Particle Architectures." *Cell Reports Physical Science* 1, 100137. https://doi.org/10.1016/j.xcrp.2020.100137.

Coupled Electrochemical-Mechanical Formulation

Governing Equations

Electrochemistry Model

$[Li]$

- **Lithium transport → lithium concentration** $[\boldsymbol{Li}]$

$$[\dot{Li}] + \nabla \cdot \boldsymbol{J} = 0 \quad in\ \Omega \quad (Similar\ to\ a\ transient\ heat\ equation)$$

Fickian diffusion: $\boldsymbol{J} = -\nabla(D[Li])$

Φ_{NMC}

- **Solid-phase electrostatic potential →** $\boldsymbol{\Phi_{NMC}}$

$$\nabla \cdot (\kappa \nabla \Phi_{NMC}) = 0 \quad in\ \Omega \quad (Poisson\ equation)$$

Mechanics Model

$\boldsymbol{u}$

- **Mechanics →** $\boldsymbol{u}$

$$\nabla \cdot \boldsymbol{\sigma} = \boldsymbol{0} \quad in\ \Omega \quad (Balance\ of\ linear\ momentum)$$

Stress: $\boldsymbol{\sigma} = \mathbb{C}\boldsymbol{\epsilon}^e$

$$\boldsymbol{\epsilon}^e = \boldsymbol{\epsilon} - \boldsymbol{\epsilon}^{[Li]}$$

Electrochemistry Boundary Condition (BC): Butler-Volmer Relation

- **Lithium transport → intercalated lithium concentration** $[Li]$

BC: $$\nabla(D[Li]) \cdot \boldsymbol{n} = -\frac{i}{F} \quad on\ \Gamma_h$$

- **Solid-phase electrostatic potential →** Φ_{NMC}

BC: $$\kappa \nabla \Phi_{NMC} \cdot \boldsymbol{n} = -i \quad on\ \Gamma_h$$

- **Butler-Volmer coupling**

BC: $$i = i_0 \left[\exp\left(\frac{\alpha_a \eta F}{RT}\right) - \exp\left(-\frac{\alpha_c \eta F}{RT}\right) \right] \quad on\ \Gamma_h$$

$$\eta([Li], \Phi_{NMC}) = \Phi_{NMC} - \Phi_{el} - E^{eq}\left(\frac{[Li]}{[Li]_{max}}\right)$$

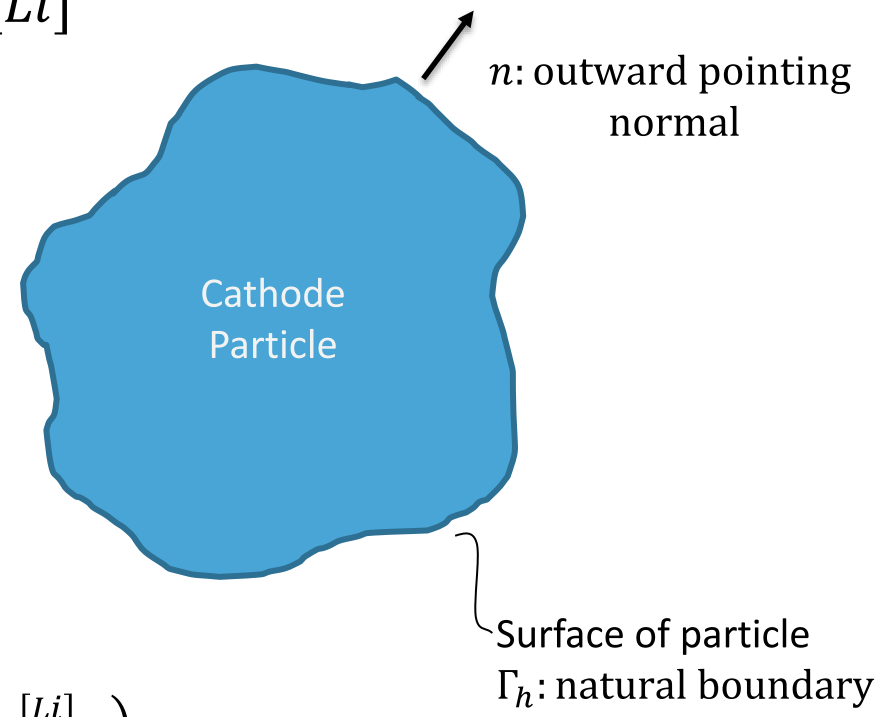

Reproducing Kernel Particle Method (RKPM)

Reproducing Kernel (RK) Approximation

RK Approximation:

$$u(\boldsymbol{x}) \approx u^h(\boldsymbol{x}) = \sum_{I=1}^{NP} \Psi_I(\boldsymbol{x}) d_I$$

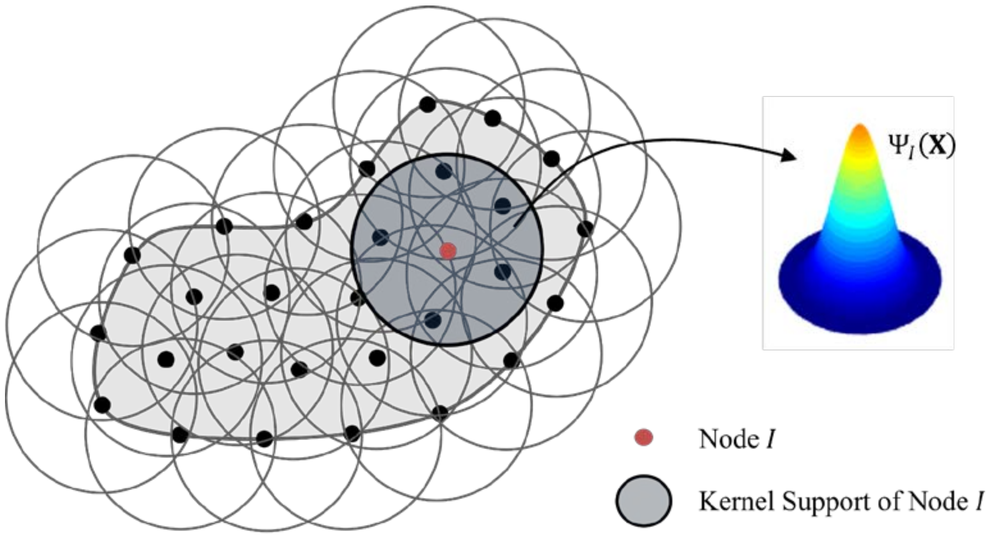

Shape Function Construction: $\Psi_I(\boldsymbol{x})$

Strategic Correction of Kernel Functions, ϕ_a :

$$\Psi_I(\boldsymbol{x}) = C(\boldsymbol{x}; \boldsymbol{x} - \boldsymbol{x}_I)\phi_a(\boldsymbol{x} - \boldsymbol{x}_I) = \left(\sum_{|\boldsymbol{\alpha}| \le n} (\boldsymbol{x} - \boldsymbol{x}_I)^{\boldsymbol{\alpha}}\, b_{\boldsymbol{\alpha}}(\boldsymbol{x})\right) \phi_a(\boldsymbol{x} - \boldsymbol{x}_I)$$

$$\Psi_I(\boldsymbol{x}) \equiv \boldsymbol{H}^T(\boldsymbol{x} - \boldsymbol{x}_I)\boldsymbol{b}(\boldsymbol{x})\phi_a(\boldsymbol{x} - \boldsymbol{x}_I)$$

$$\boldsymbol{H}^T(\boldsymbol{x} - \boldsymbol{x}_I) = [1, (x_1 - x_{1I}), (x_2 - x_{2I}), (x_3 - x_{3I}), \dots, (x_3 - x_{3I})^n]$$

Reproducing Conditions:

$$\sum_{\mathrm{I}=1}^{NP} \Psi_I(\boldsymbol{x})\boldsymbol{x}_I^{\boldsymbol{\alpha}} = \boldsymbol{x}^{\boldsymbol{\alpha}}, \qquad |\boldsymbol{\alpha}| \le n \quad OR \quad \sum_{I=1}^{NP} \Psi_I(\boldsymbol{x})(\boldsymbol{x} - \boldsymbol{x}_I)^{\boldsymbol{\alpha}} = \delta_{0\boldsymbol{\alpha}}, |\boldsymbol{\alpha}| \le n$$

$$\boldsymbol{b}(\boldsymbol{x}) = \boldsymbol{M}^{-1}(\boldsymbol{x})\boldsymbol{H}(\boldsymbol{0}), \;\; where\; \mathbf{M}(\boldsymbol{x}) = \sum_{I=1}^{NP} \mathrm{H}(\boldsymbol{x} - \boldsymbol{x}_I)\mathrm{H}^{\mathrm{T}}(\boldsymbol{x} - \boldsymbol{x}_I)\phi_a(\boldsymbol{x} - \boldsymbol{x}_I)$$

$$\Psi_I(\boldsymbol{x}) = \boldsymbol{H}^T(\boldsymbol{0})\boldsymbol{M}^{-1}(\boldsymbol{x})\boldsymbol{H}(\boldsymbol{x} - \boldsymbol{x}_I)\phi_a(\boldsymbol{x} - \boldsymbol{x}_I)$$

4. Liu, W.K., S. Jun, S. Li, J. Adee, T. Belytschko. 1995. "Reproducing kernel particle methods for structural dynamics." *Int J Numer Methods Eng* 38(10): 1655-1679. https://doi.org/10.1002/nme.1620381005.
5. Chen, J.S., C. Pan, C-T Wu, W.K. Liu. 1996. "Reproducing kernel particle methods for large deformation analysis of non-linear structures." *Comput Methods Appl Mech Eng* 139(96): 195-227. https://doi.org/10.1016/S0045-7825(96)01083-3.

Linear Patch Test for Coupled Problem

Linear Patch Test for Coupled Problem

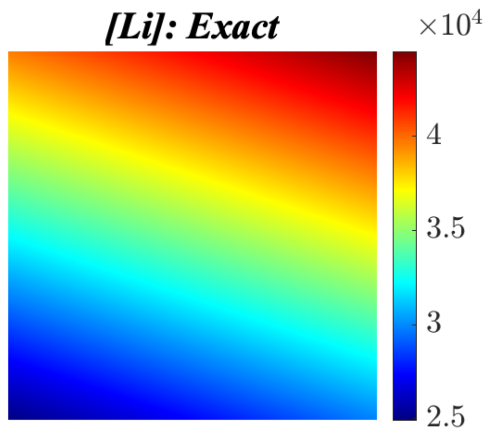

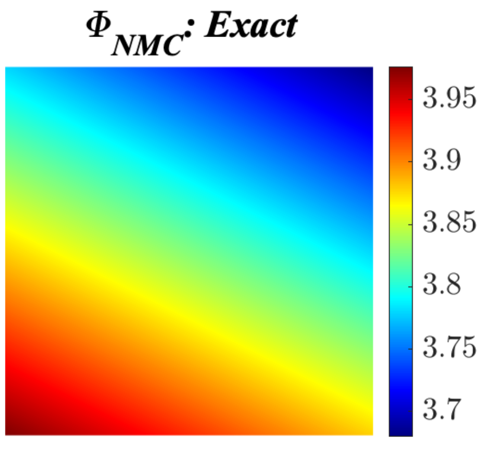

Field	$\mathbf{L_2}$ Norm	$\mathbf{H^1}$ Seminorm
$[Li]$	$5.041e-07$	$8.692e-10$
Φ_{NMC}	$6.604e-12$	$2.762e-12$

- Designing Mixed BCs (applied as Natural BCs)
  - $\mathrm{BC}_{[\mathrm{Li}]}$: $\boldsymbol{\nabla}(D[Li]) \cdot \boldsymbol{n} = -\frac{i}{F} \quad on\ \Gamma_{h_{[Li]}}$
    $$\Rightarrow \boldsymbol{\nabla}(D[Li]) \cdot \boldsymbol{n} = -\frac{i}{F} + \frac{i^p}{F} + \boldsymbol{\nabla}(D[Li]^p) \cdot \boldsymbol{n} \quad on\ \Gamma_{h_{[Li]}}$$
  - BC_{Φ}: $\kappa \boldsymbol{\nabla} \Phi_{NMC} \cdot \boldsymbol{n} = -i \quad on\ \Gamma_{h_{\Phi_{\mathrm{NMC}}}}$
    $$\Rightarrow \kappa \boldsymbol{\nabla} \Phi_{NMC} \cdot \boldsymbol{n} = -i + i^p + \kappa \boldsymbol{\nabla} \Phi_{NMC}^p \cdot \boldsymbol{n} \quad on\ \Gamma_{h_{\Phi_{NMC}}}$$

Note: We **recover the original governing equations** once convergence is reached.

Note: A **mixed type boundary condition** is maintained through Butler-Volmer coupling.
$i^p = i\left([Li]^p, \Phi_{NMC}^p\right)$

Introducing Weak and Strong Discontinuities to the RK Approximation Space

Kernel Function Modifications for Grain Boundaries: $\max[\tanh(dist), 0]$

Case 1: Scaling with node on boundary

Weak discontinuity introduced only for $\Psi_{Boundary}$

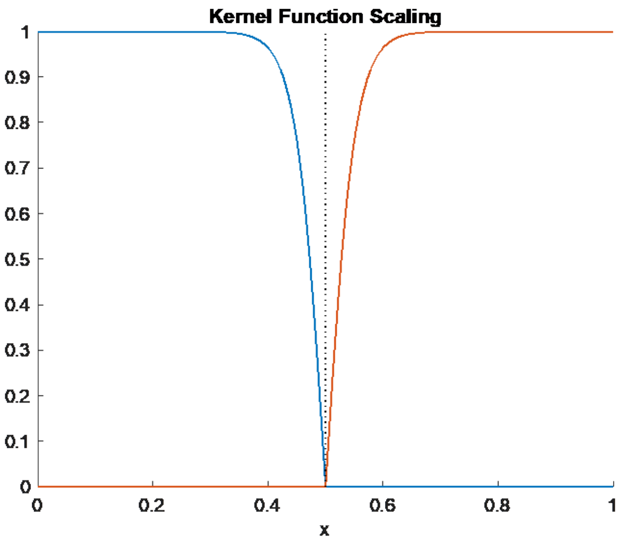

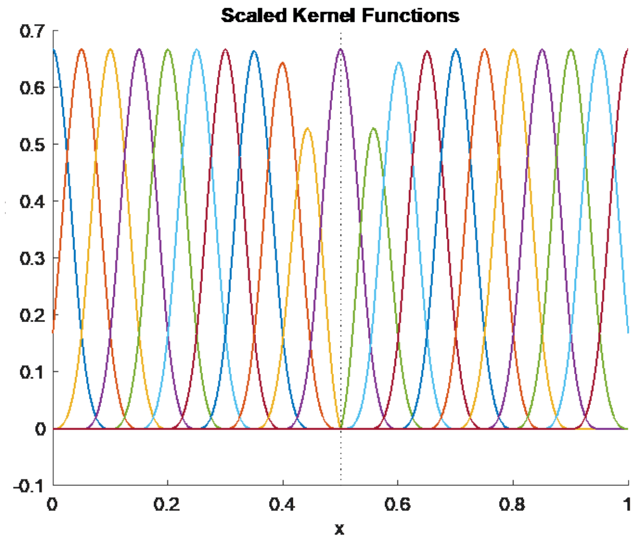

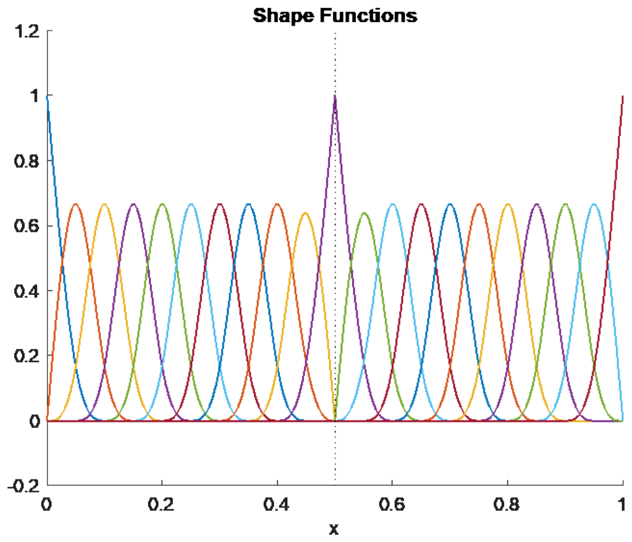

Case 2: Scaling with no node on boundary

Strong discontinuity introduced only for $\Psi_{Boundary}$

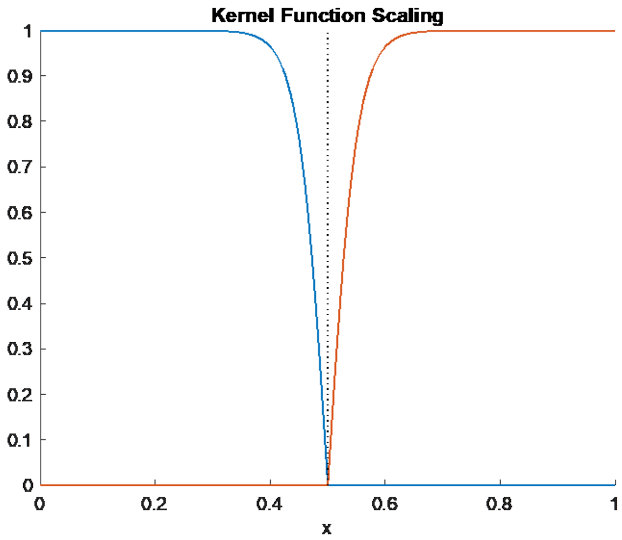

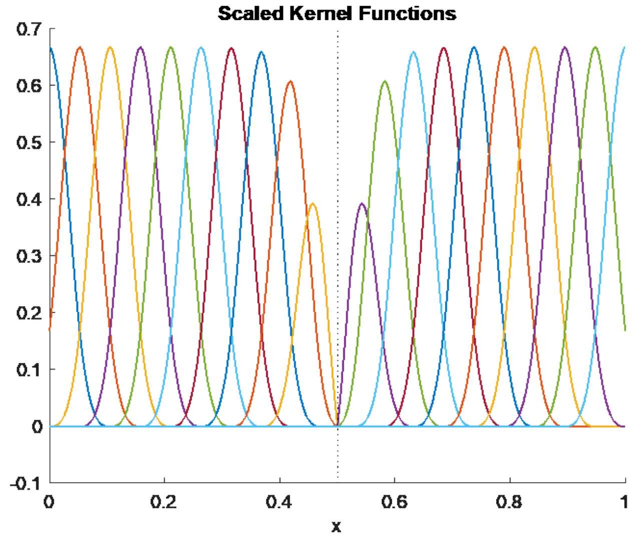

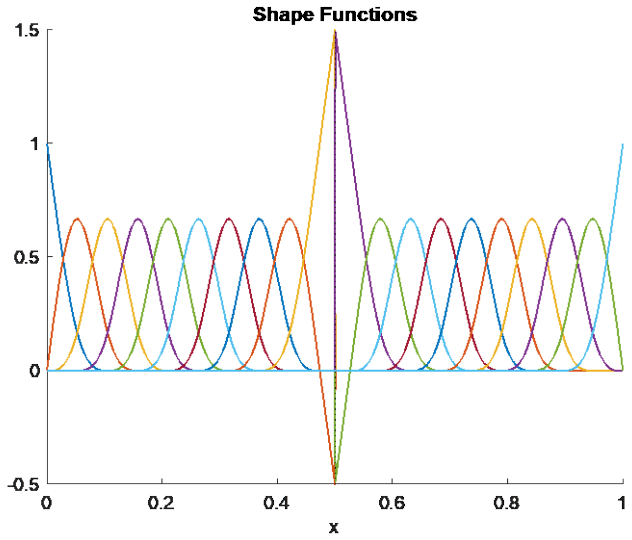

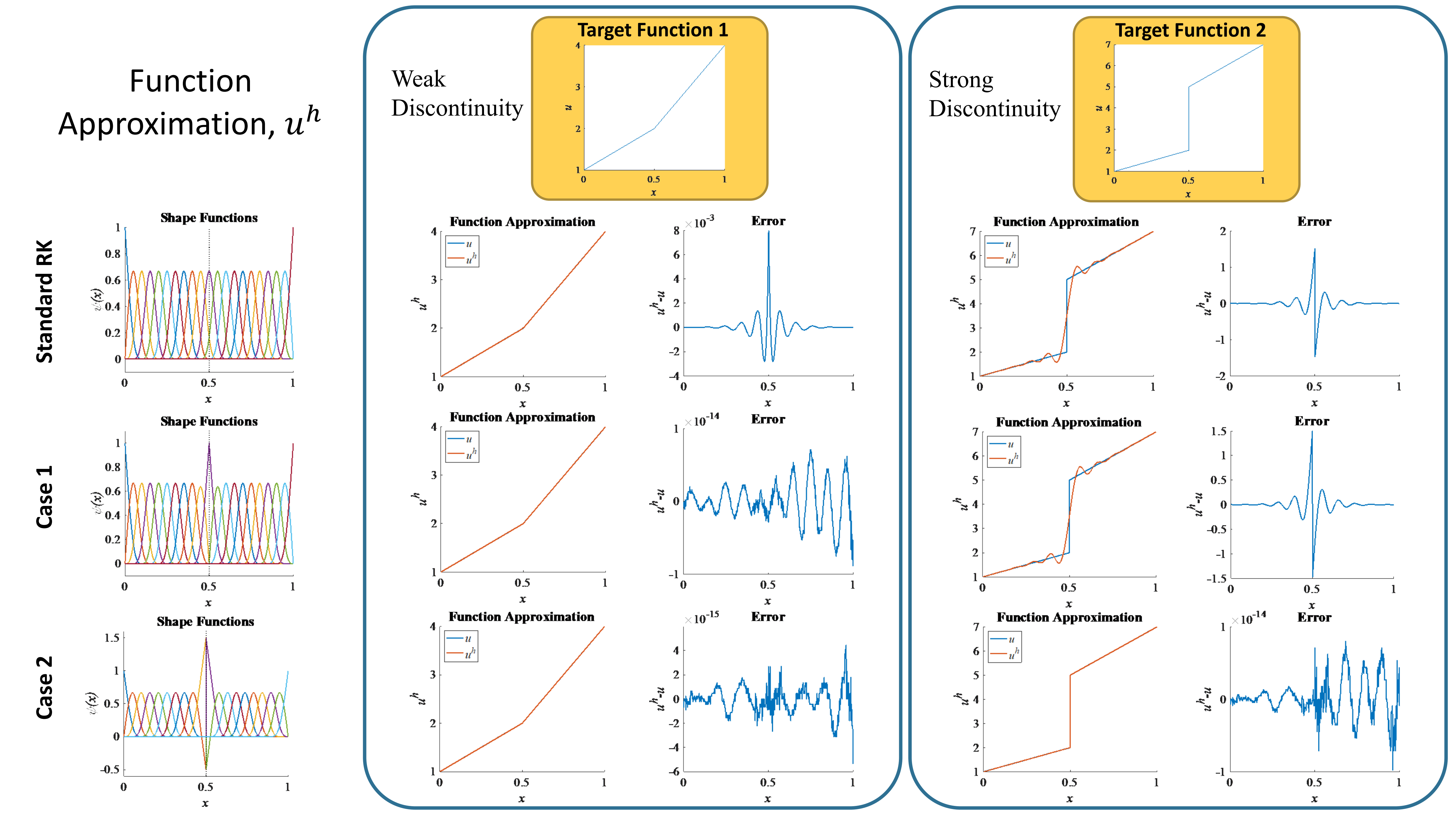
Function Approximation, u^h
Standard RK
Case 1
Case 2
Shape Functions
Weak Discontinuity
Target Function 1
Strong Discontinuity
Target Function 2
Function Approximation
Error
u
u^h
u^h-u
$\psi(x)$
x

Image-based Modeling

From Pixels to Nodes

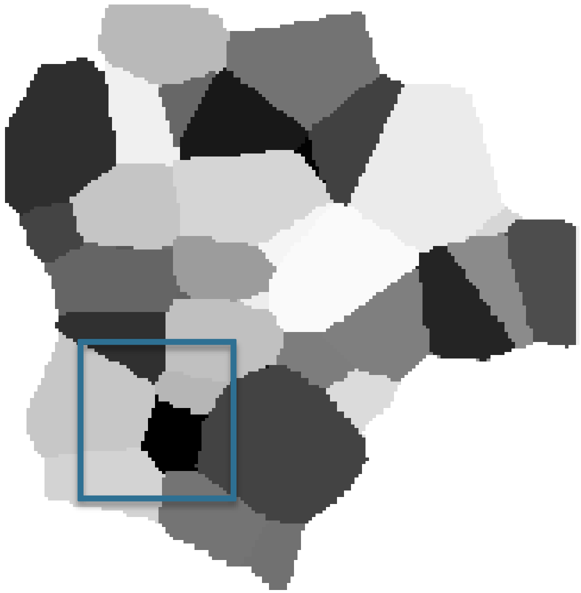

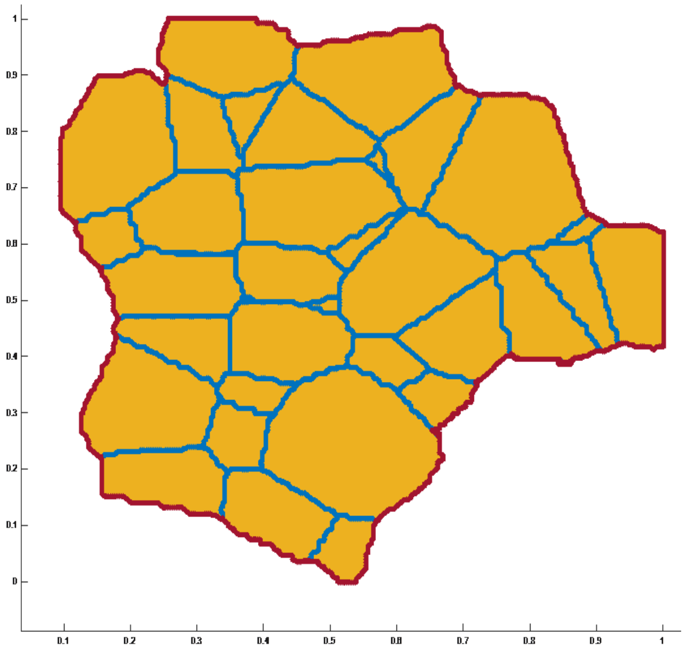

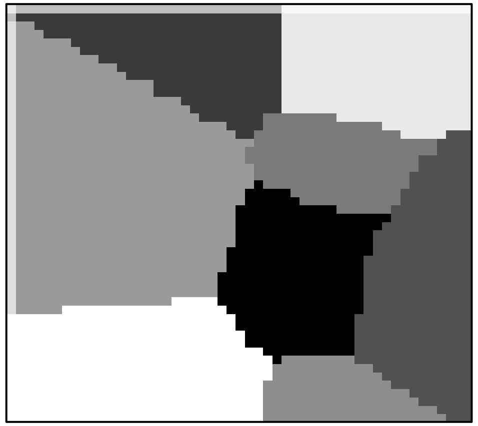

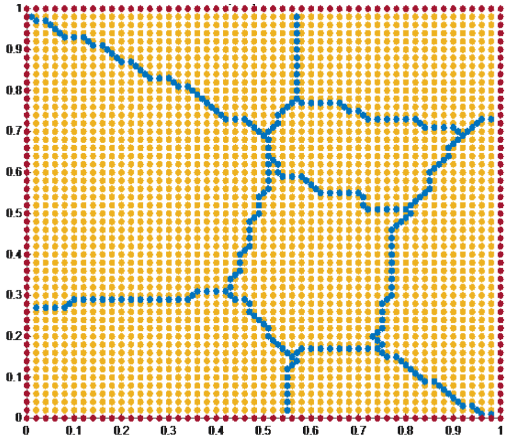

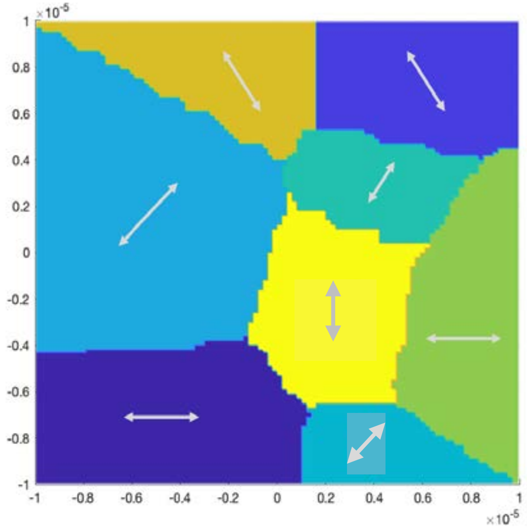

Standard RKPM

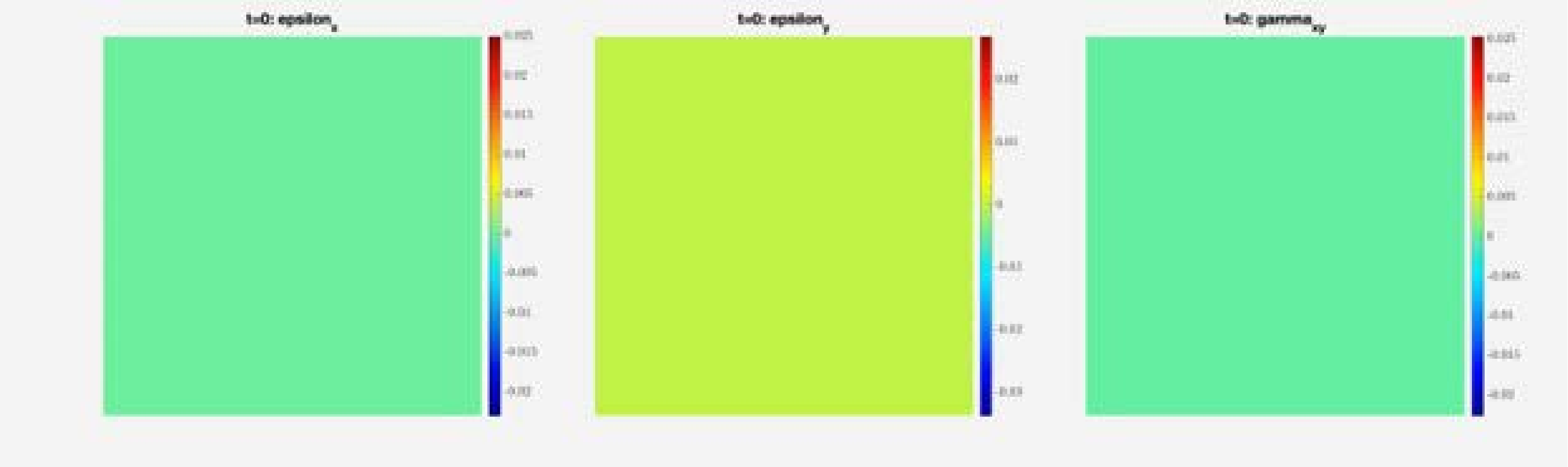

RKPM with Kernel Scaling on Grain Boundaries

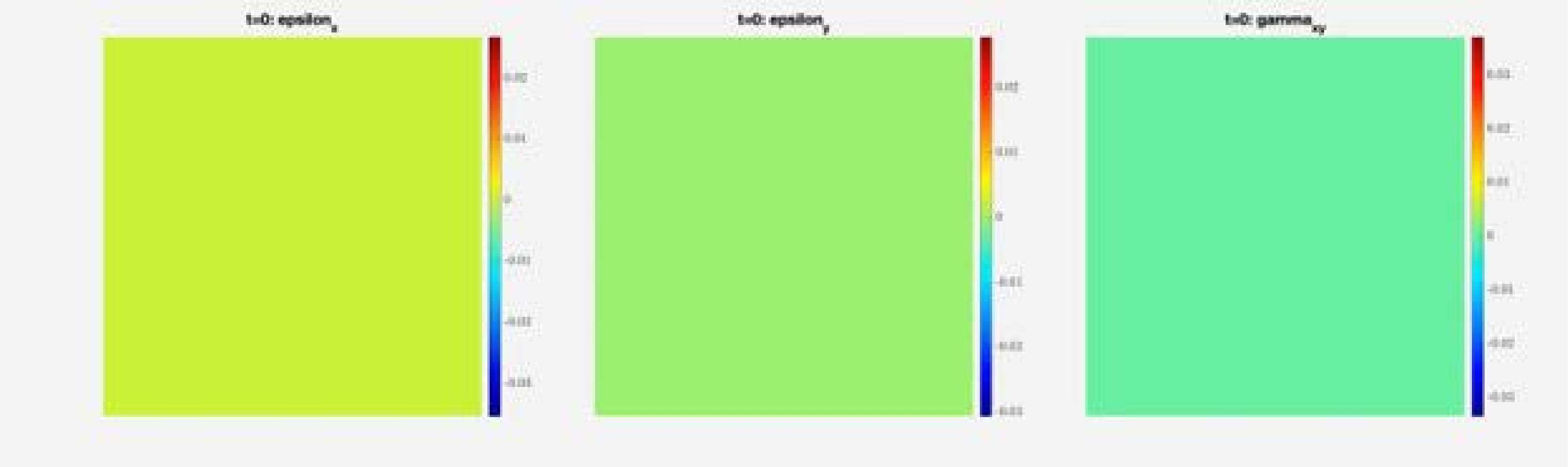

Neural Network Enhanced Reproducing Kernel Approximation

Neural Network Enhanced Reproducing Kernel (NN-RK) Approximation

Solution decomposition

$$\mathbf{u}^h = \tilde{\mathbf{u}}^h + \hat{\mathbf{u}}^h$$

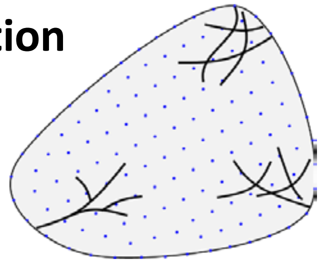

<u>**Smooth solution approximation**</u>

$$\tilde{\mathbf{u}}^h(\mathbf{X}) \approx \mathbf{u}^{RK}(\mathbf{X}) = \sum_{I=1}^{NP} \Psi_I(\mathbf{X})\mathbf{d}_I$$

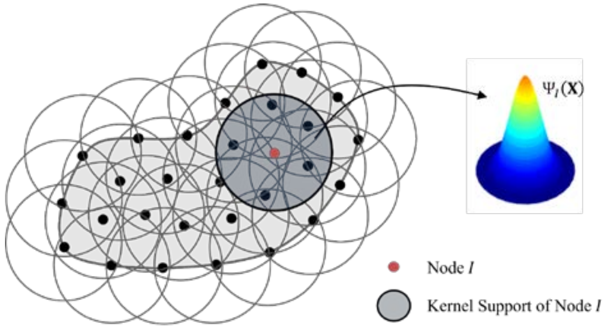

<u>**Neural Network (NN) Enrichment**</u>

$$\hat{\mathbf{u}}^h(\mathbf{x}) \approx \mathbf{u}^{NN}(\mathbf{X}) = \sum_{I=1}^{NB} b_I(\mathbf{X}; \mathbf{W})$$

Neural network (NN) approximation

$$u^{NN}(\mathbf{x}) = \sum_{B=1}^{N_B} b_B^{NN}(\mathbf{x}; \mathbf{W}_B)$$

- b_B^{NN}: block-level NN approximation

Block-level NN approximation

$$b_B^{NN}(\mathbf{x}; \mathbf{W}) = \sum_{K=1}^{N_K} \hat{\phi}_{KB}\left(\mathbf{y}(\mathbf{x}; \mathbf{W}_B^L), \mathbf{W}_{KB}^S\right) p(\mathbf{x}; \mathbf{W}_{KB}^P)$$

- NK: the number of NN kernels per block

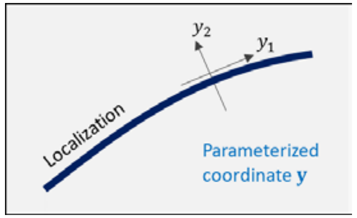

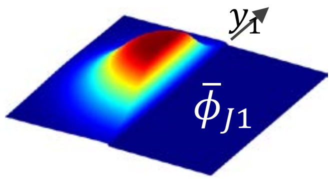

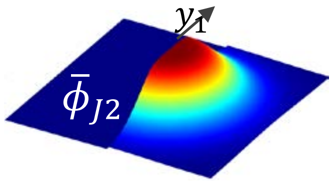

NN Kernel function captures
- Location and orientation of localization
- Shape of solution transition

NN Polynomial introduces
- Monomial completeness for further accuracy

- $\mathbf{W}^L$: NN weight set controlling the location and orientation of the kernel.
- $\mathbf{W}^S$: NN weight set controlling the shape of transition.

- $\mathbf{W}^P$: NN monomial coefficient set

* The NN control parameters $\mathbf{W}^L$, $\mathbf{W}^S$, and $\mathbf{W}^P$ are ***automatically*** determined via loss function minimization.

6. Baek, J., J.S. Chen, K. Susuki. 2022. "A neural network-enhanced reproducing kernel particle method for modeling strain localization." *Int J Numer Methods Eng* 123(18): 4422-4454. https://doi.org/10.1002/nme.7040.

Block-Level Neural Network Architecture

A block-level neural network is a modified deep neural network with ***increased interpretability***.

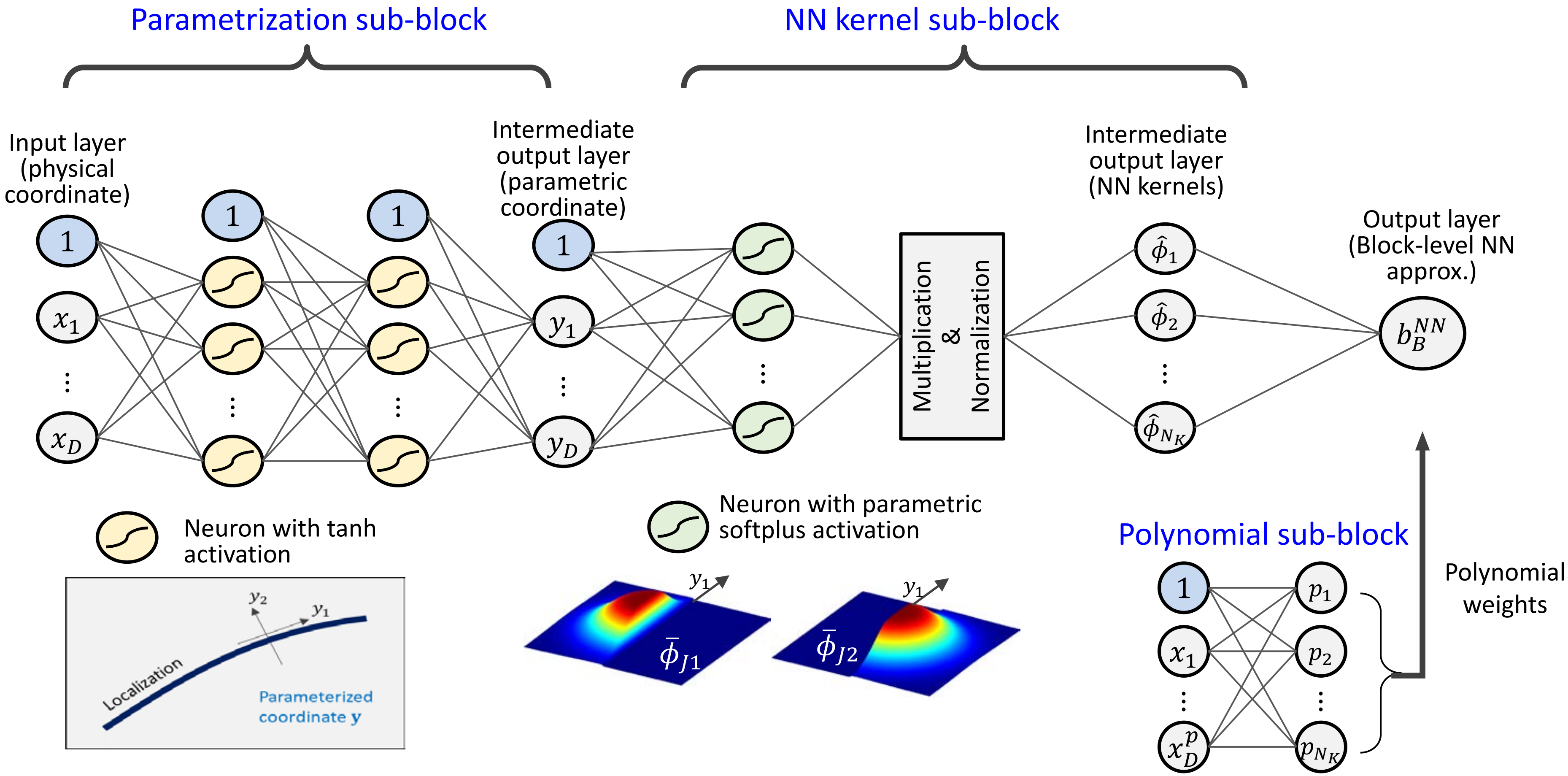

6. Baek, J., J.S. Chen, K. Susuki. 2022. "A neural network-enhanced reproducing kernel particle method for modeling strain localization." *Int J Numer Methods Eng* 123(18): 4422-4454. https://doi.org/10.1002/nme.7040.

NN Kernel Function Controlled by $\mathbf{W}^S$

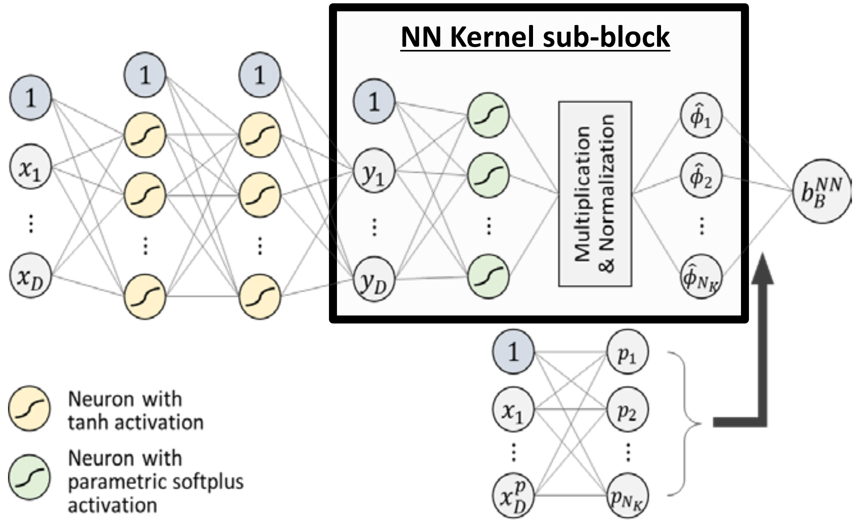

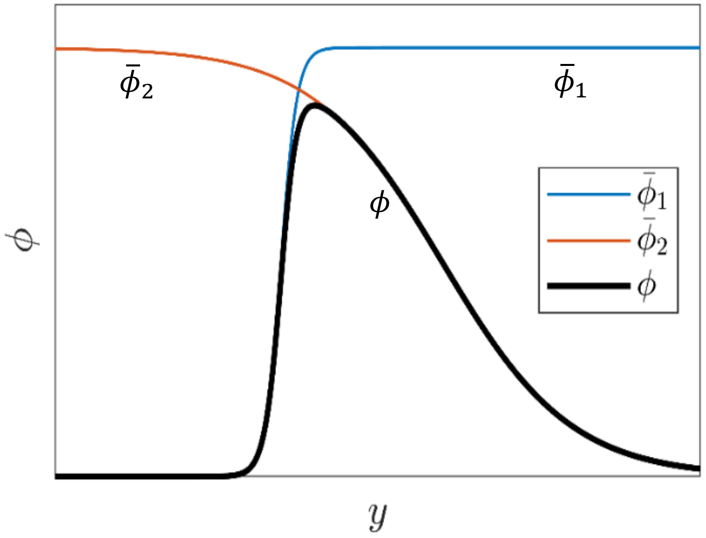

NN Kernel Function

$$\phi(y;\mathbf{W}^S_{KB}) = \prod_{i=1}^{2} \underbrace{\bar{\phi}\left(z_i\left(y,\bar{y}_i^{KB},c_i^{KB}\right);\beta_i^{KB}\right)}_{\text{Regularized step functions}}$$

Regularized Step Functions

$$\bar{\phi}(z_i;\beta_i) \equiv S\left(z_i+\frac{1}{2};\beta_i\right) - S\left(z_i-\frac{1}{2};\beta_i\right)$$

Where $z_i = (-1)^i\,(y-\bar{y}_i)/c_i$, $i = 1, 2$

$$S(z;\beta) = \frac{1}{\beta}\log\left(1+e^{\beta z}\right)$$

(parametric softplus function)

6. Baek, J., J.S. Chen, K. Susuki. 2022. “A neural network-enhanced reproducing kernel particle method for modeling strain localization.” *Int J Numer Methods Eng* 123(18): 4422-4454. https://doi.org/10.1002/nme.7040.

Neural Network Kernel Function Controlled by $\mathbf{W}^S$

NN Control Parameter $\bar{y}$

Domain of influence

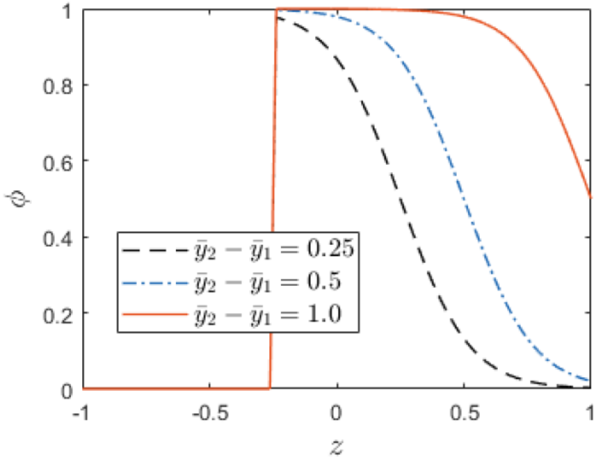

NN Control Parameter c

Transition of NN kernel function

NN kernel function

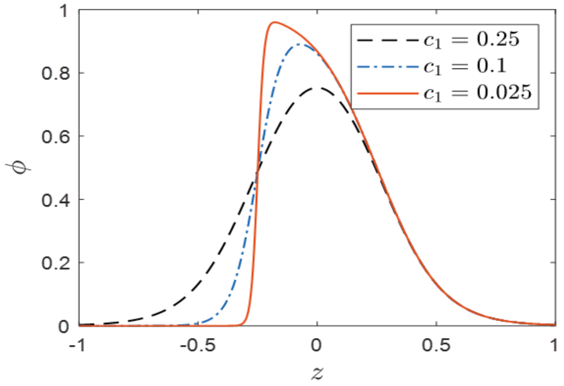

NN kernel function derivatives

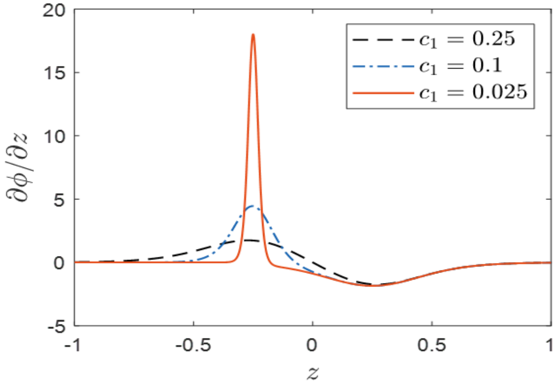

NN Control Parameter β

Transition of NN kernel function derivative

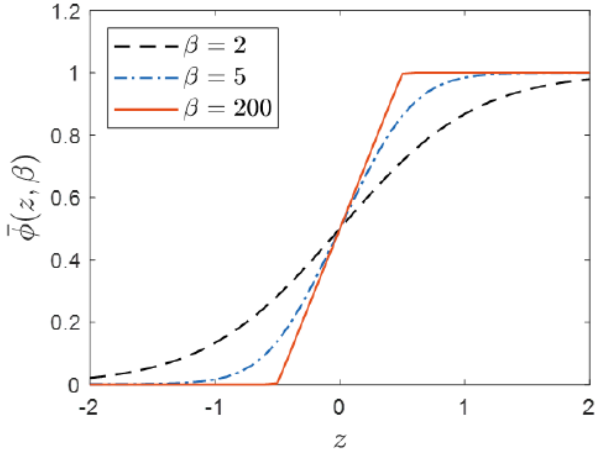

6. Baek, J., J.S. Chen, K. Susuki. 2022. "A neural network-enhanced reproducing kernel particle method for modeling strain localization." *Int J Numer Methods Eng* 123(18): 4422-4454. https://doi.org/10.1002/nme.7040.

Convergence Performance for Function Evaluation: (1) Influence of the Number of Neurons (N_{NR})

Average rate of convergence: 2.282

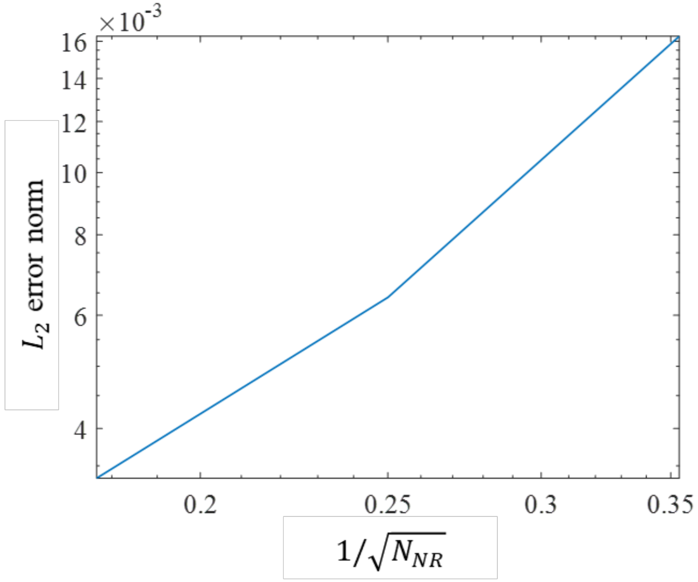

Number of block $N_B = 1$
Number of NN kernel per block $N_K = 4$

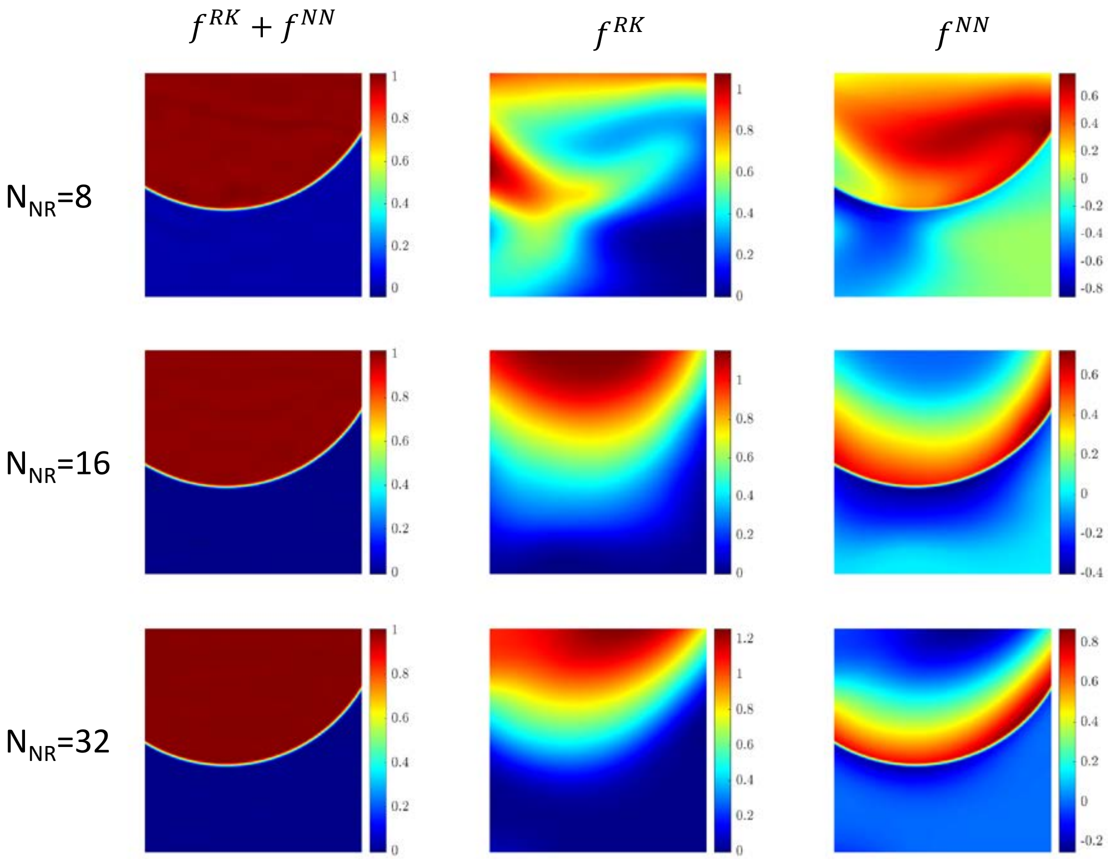

6. Baek, J., J.S. Chen, K. Susuki. 2022. "A neural network-enhanced reproducing kernel particle method for modeling strain localization." *Int J Numer Methods Eng* 123(18): 4422-4454. https://doi.org/10.1002/nme.7040.

Convergence Performance for Function Evaluation: (2) Influence of the number of NN Blocks (N_B)

Average rate of convergence: 3.578

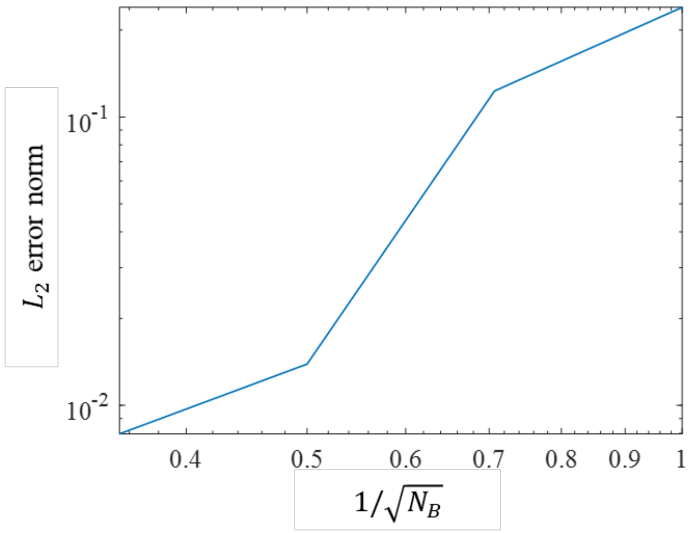

Number of neurons $N_{NR} = 32$
Number of NN kernel per block $N_K = 4$

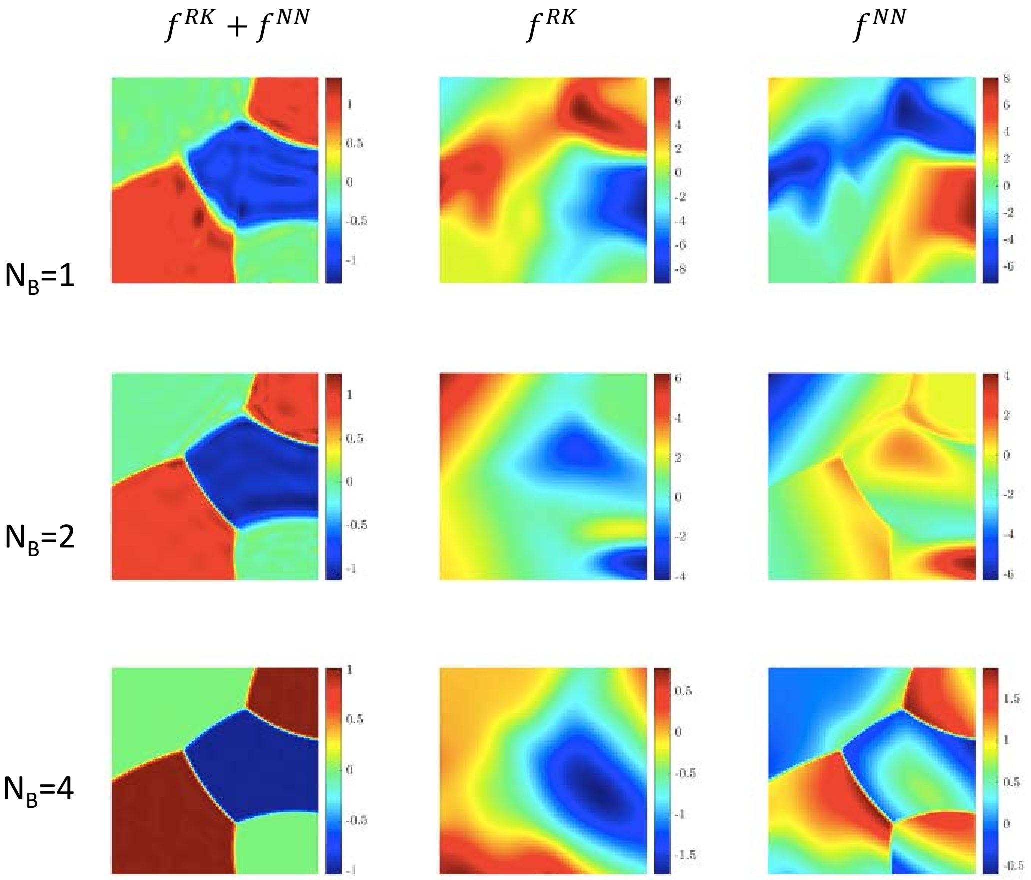

6. Baek, J., J.S. Chen, K. Susuki. 2022. "A neural network-enhanced reproducing kernel particle method for modeling strain localization." *Int J Numer Methods Eng* 123(18): 4422-4454. https://doi.org/10.1002/nme.7040.

Damage Evolution

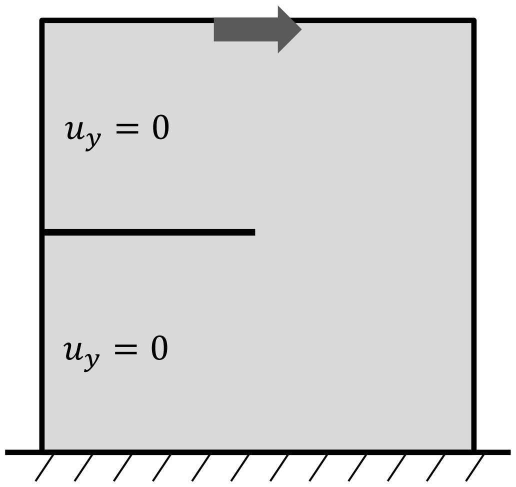

$$\min \Pi = \frac{1}{2}\int_{\Omega}(g(\eta)\psi^{+} + \psi^{-})d\Omega + p\int_{\Omega}\eta^{2}d\Omega + \Pi^{ebc}$$

Damage $\eta = \dfrac{\kappa}{\kappa + p}$ $\kappa = \psi^{+} - \psi^{c}$ $p = G_c/\ell$

$$g(\eta) = (1-\eta)^2$$

$$\psi^{+} = \frac{1}{2}\lambda\langle tr\varepsilon_i\rangle^2 + \mu\varepsilon_i^{+}\varepsilon_i^{+}$$

$$\psi^{-} = \frac{1}{2}\lambda((tr\varepsilon_i)^2 - \langle tr\varepsilon_i\rangle^2) + \mu\varepsilon_i^{-}\varepsilon_i^{-}$$

$$\langle\cdot\rangle = \max(0,\cdot)$$

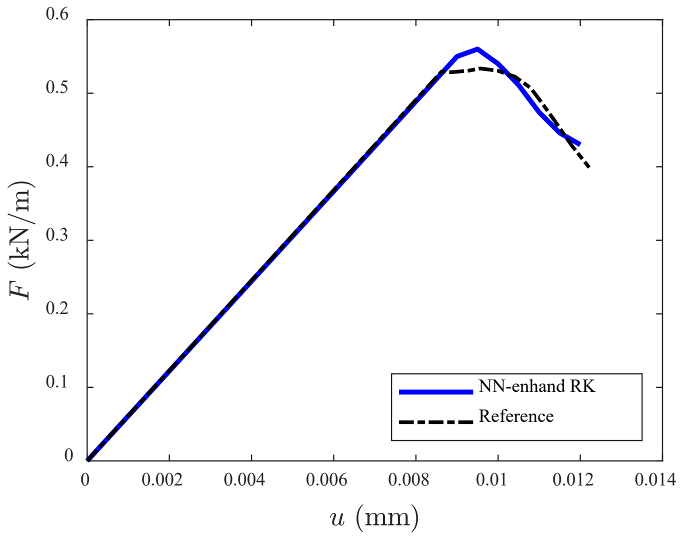

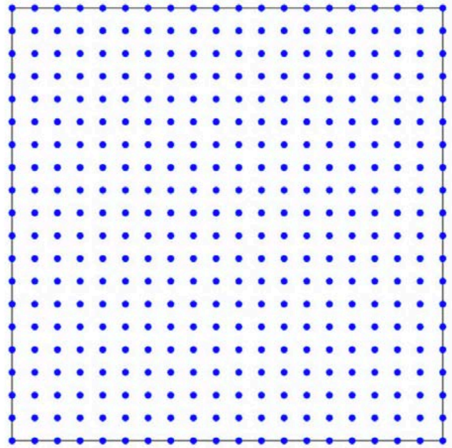

- 256 RK particles (16X16) are used with 512 RK coefficients.
- 3 NN blocks are used with 540 total unknown weights and biases.
- Visibility criteria with diffraction is applied to the RK shape functions around the area of pre-existing crack.

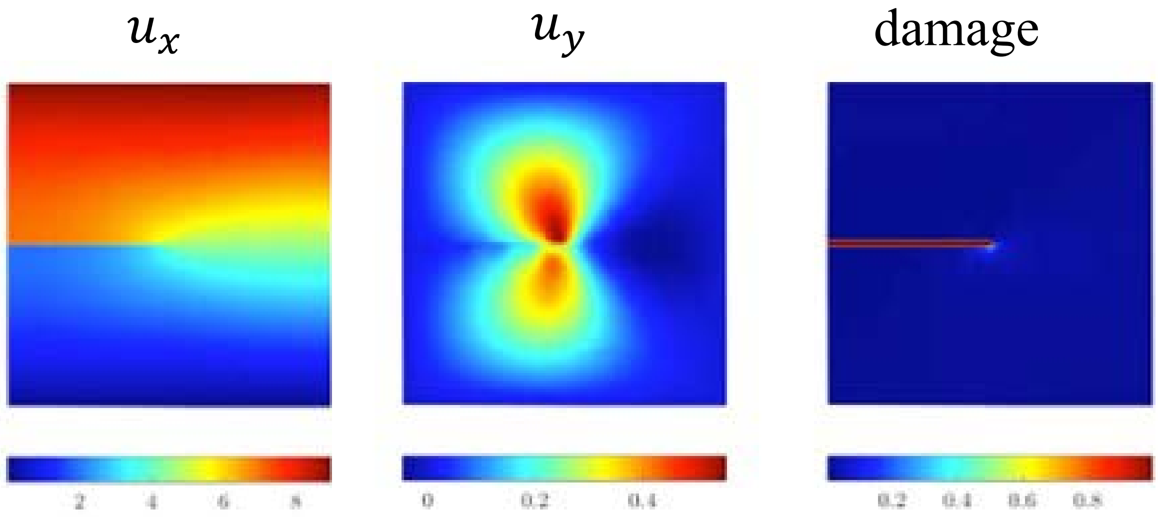

6. Baek, J., J.S. Chen, K. Susuki. 2022. "A neural network-enhanced reproducing kernel particle method for modeling strain localization." *Int J Numer Methods Eng* 123(18): 4422-4454. https://doi.org/10.1002/nme.7040.
7. Miehe C, Hofacker M, Welschinger F. A phase field model for rate-independent crack propagation: robust algorithmic implementation based on operator splits. Comput Methods Appl Mech Eng. 2010;199(45):2765-2778. https://doi.org/10.1016/j.cma.2010.04.011

Mixed-mode Fracture of a Doubly Notched Crack Branching

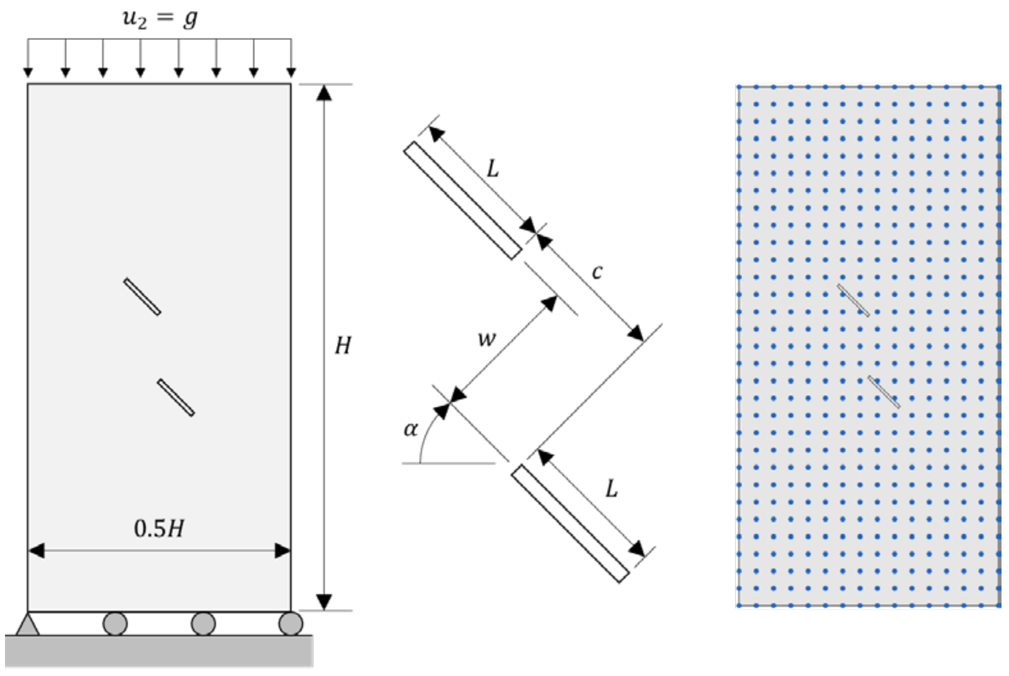

(a) (b) (c)

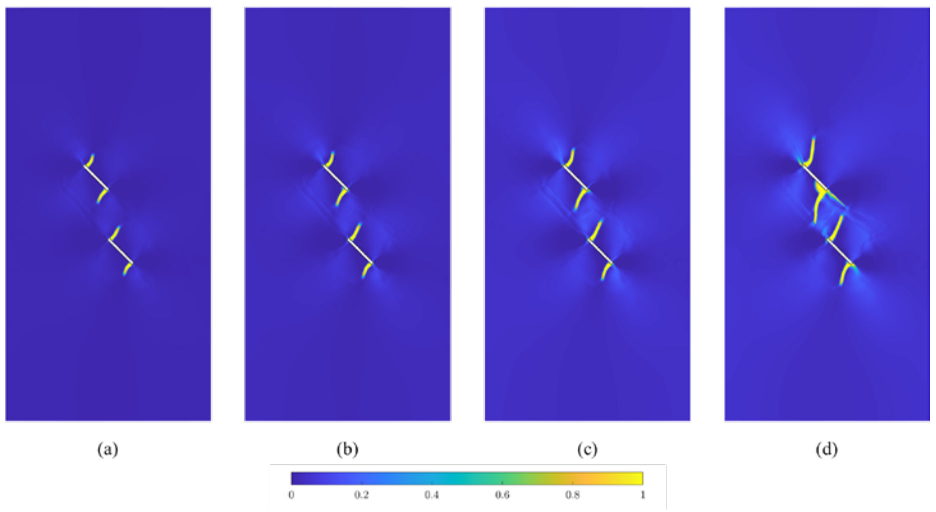

(a) (b) (c) (d)

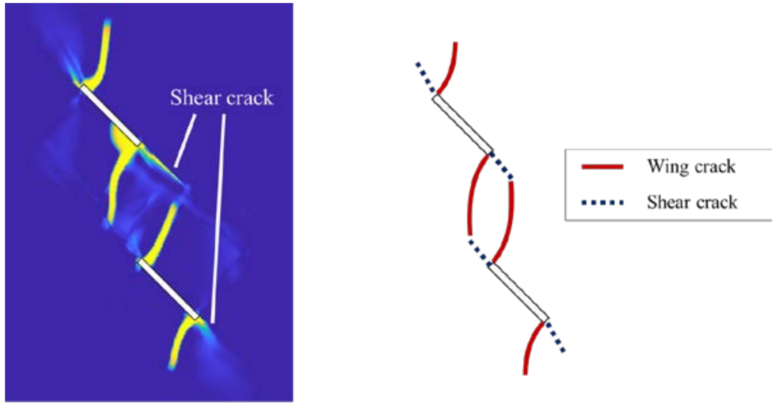

(a) (b)

NN-RKPM Experiment (reference)

8. Baek, J., Chen, J. S., "A Neural Network-Based Enrichment of Reproducing Kernel Approximation for Modeling Brittle Fracture", submitted, Computer Methods in Applied Mechanics and Engineering, 2023
9. Bobet, A., H.H. Einstein, Numerical modeling of fracture coalescence in a model rock material, Int. J. Fract. 92 (1998) 221–252. https://doi.org/https://doi.org/10.1023/A:1007460316400

Conclusions and Future Work

Conclusions:

- A coupled linear patch test was designed and passed for the electrochemical model.
- Through kernel function scaling and strategic RK node placement, weak and strong discontinuities along grain boundaries were introduced in a flexible manner.
- Image-based modeling techniques were leveraged for realistic model construction.
- NN enhancement increased localization accuracy in homogeneous materials without model refinement.

Thank you

Kristen Susuki – ksusuki@ucsd.edu

This work was authored in part by the National Renewable Energy Laboratory, operated by Alliance for Sustainable Energy, LLC, for the U.S. Department of Energy (DOE) under Contract No. DE-AC36-08GO28308. Funding provided by U.S. Department of Energy Office of Energy Efficiency and Renewable Energy. The views expressed in the article do not necessarily represent the views of the DOE or the U.S. Government. The U.S. Government retains and the publisher, by accepting the article for publication, acknowledges that the U.S. Government retains a nonexclusive, paid-up, irrevocable, worldwide license to publish or reproduce the published form of this work, or allow others to do so, for U.S. Government purposes.